Exploring the structure of glass-forming liquids using high energy X-ray diffraction, containerless methodology and molecular dynamics simulation☆

Martin Wilding[a,g,*], Chris Benmore[b], Rick Weber[b,c], Oliver Alderman[b,c], Anthony Tamalonis[c], Paul F. McMillan[d], Mark Wilson[e], Mauro C.C. Ribiero[f], John Parise[g]

[a] Materials and Engineering Research Institute, Sheffield Hallam University, Howard Street, Sheffield W1 1WB, UK
[b] X-ray science division, Advanced Photon Source, Argonne National Laboratory, Argonne, IL 60439, USA
[c] Materials Development Inc. Arlington Heights, IL 60004, USA
[d] Department of Chemistry, University College London, 20 Gordon Street, London WC1H 0AJ, UK
[e] Department of Chemistry, Physical and Theoretical Chemistry Laboratory, University of Oxford, South Parks Road, Oxford OX1 3QZ, UK
[f] Laboratório de Espectroscopia Molecular, Instituto de Química, Universidade de São Paulo. Av. Prof. Lineu Prestes 748, São Paulo 05508-000, Brazil
[g] Department of Geosciences, Stony Brook University, Stony Brook, NY 11794-2100, USA

ABSTRACT

High energy X-ray diffraction can be combined with containerless techniques to provide information on the atomic arrangements in glass-forming liquids in stable and metastable regimes. The high incident energies provide bulk diffraction data to high values of scattering vector which enables significantly more robust analysis of the local and medium-range order that influences important physical properties such as viscosity and crystal nucleation.

These combined techniques have been applied to a range of oxide liquids. In this contribution we illustrate addition of further dimensions to phase space by controlling the partial pressure of oxygen that permits the study liquids containing iron. The advantages of rapid data acquisition are also demonstrated in a study of tellurite glass-forming systems where a transition from ergodic to non-ergodic regimes in the deeply supercooled liquid is shown. Finally we demonstrate how descriptions of the liquid structure can be developed by combining HEXRD with molecular dynamics simulations.

1. Introduction

The physical behaviour of liquids is strongly influenced by the liquid viscosity which controls the liquid dynamics and crystallisation behaviour. The dynamic properties can be related to the atomic scale arrangements through the concepts of "strong" *vs* "fragile liquid behaviour fragility developed and popularised by Angell [1] correlated with the configurational entropy (S_{conf}) as expressed by the Adam-Gibbs model of structural relaxation [2]. In the classic master diagram, the temperature-dependent liquid viscosity (log η) is plotted against the inverse temperature normalised to the calorimetric glass transition temperature (T_g) for different materials. Glass-forming liquids that exhibit linear log η *vs* T_g/T Arrhenius law behaviour are classified as "strong" and are associated with either small changes in local structure or high barriers between different configurations as a function of temperature. Increasing curvature in the log η *vs* T_g/T plot denotes

increasing fragility and a larger number of configurational states accessible as a function of temperature. These correlations demonstrate the need for understanding temperature-dependent changes in the local to medium-range structure of stable and supercooled liquids to examine their glass-forming *vs* recrystallization behaviour, along with the quenchability of different structural states as a function of the cooling rate. Establishing such relations between liquid structures and dynamic relaxation problems remains a significant challenge for liquid and amorphous state science that can be addressed by high energy X-ray diffraction experiments carried out on stable to deeply supercooled liquids using containerless levitation techniques. Here we present some key results that illustrate and develop applications of these combined techniques, coupled with MD simulation results, to a range of key systems for materials science and geochemical studies.

Diffraction studies with short wavelength radiation approaching that of interatomic spacing provides a powerful method of determining

---

☆ Presented at the "Frontiers in Glass Science" Symposium 7th International Congress on Ceramics, Foz do Iguaçu, Brazil 17-21st June 2018.
* Corresponding author at: Materials and Engineering Research Institute, Sheffield Hallam University, Howard Street, Sheffield W1 1WB, UK.
 E-mail address: m.wilding@shu.ac.uk (M. Wilding).

structural configurations in liquids and amorphous solids [3]. The structural data are typically presented in terms of pair-distribution functions, as the probability of finding specified sets of atoms at a radial distance from each other, and the data exhibit a series of broad peaks at characteristic distances that for multicomponent systems represent overlapping contributions of several atom-pairs. The diffraction data are collected in reciprocal space and are presented as the total scattering structure factor S(Q) in terms of the spatial correlation vector, Q, and are then Fourier transformed into real space structural correlation functions. The S(Q) contains extending over different length scales, beginning with the first few peaks that convey information about the intermediate range order, while the local structure that is most evident in the real space transforms is evidenced by overlapping oscillations at higher Q. To fully describe the liquid or glass structural configurations it is necessary to use X-ray as well as neutron radiation probes with small wavelength to maximise the range of Q values investigated.

The scattering from liquid and amorphous materials is typically weaker than that for crystalline materials, which introduces further difficulty in establishing their structures. Determining the structures at non-ambient temperatures presents additional challenges, including the fact that the amorphous scattering will typically be dominated by the signal from any crystalline container material. Use of containerless techniques eliminates such unwanted contributions from the sample environment, and they are readily combined with high energy X-rays (> 100 eV) to carry out liquid state scattering experiments. In addition, using high energy X-rays with the higher flux available at synchrotron sources means that smaller beam sizes can be used, and data acquisition is faster, and can potentially access transient structures that may form in the supercooled regime. In this contribution we outline developments in combined high energy X-ray diffraction and containerless techniques for a series of different liquids. We also outline how classical molecular dynamics simulation methodologies can be applied to study liquid structures and used to interpret the experimental scattering data, while also allowing further exploration of parameter space and contributing to our understanding of liquid relaxation dynamics and strong *vs* fragile behaviour.

2. Experimental methods

2.1. High energy X-ray diffraction

X-rays with incident energies of > 60 keV are routinely available at third generation synchrotron X-ray sources and have been used successfully to study a wide range of liquid and amorphous materials. In the examples presented here, experiments have been performed at the Advanced Photon Source using the beamlines 11-ID-C and 6-ID-D. The systems studied to date include silicate and aluminate liquids, TiO_2, borates and, recently molten uranium oxide [4–12].

In a typical HEXRD experiment a transmission geometry is adopted [13]. The incident X-ray beam is collimated to a size of, routinely 0.5×0.5 mm and scattered X-rays detected on a vertically mounted, 2048×2048 flat plate scintillation detector. Two-dimensional liquid diffraction patterns are collected on this detector and reduced to one-dimensional patterns by integrating over all the pixels, using programs such as Fit2D [14] which also corrects for polarization effects and geometry. Parameters such as sample-detector distance and detector tilt are obtained by calibrating using a crystalline standard. The first high energy x-ray super-conducting undulator (SCU-18) was installed at sector 6 (APS) in 2017 [15] and has resulted in a substantial increase in photon flux at specific energies. The combination of high brightness and small incident beam size means that data can be collected very rapidly (full liquid diffraction patterns have been obtained in a little as 0.2 s) and offers the opportunity to study complex fragile liquids where structures change rapidly with temperature.

Amorphous or low temperature liquid samples can be placed in a thin-walled capillary. Higher temperature studies require a furnace, a bulky sample environment that will dominate the total scattering signal. The use of a furnace can be avoided if containerless techniques are used. These ample environments can be fully integrated into high energy beam lines.

2.2. Containerless techniques

The sample environment is eliminated in the containerless methodology and these techniques enable studies of the liquid state directly. In this contribution high temperature containerless techniques are discussed. For liquid with melting points > 300 °C, aerodynamic levitation furnaces can be used, whilst the acoustic levitation techniques is more applicable for lower melting point liquids and aqueous solutions. The aerodynamic levitation furnace consists of a custom designed, water-cooled conical nozzle in which a bead of ceramic precursor is levitated by a gas jet. The bead is heated from above by 400 W CO_2 laser [13]. The temperature is monitored by pyrometer. The entire levitation furnace is enclosed in a stainless steel shroud with access ports for video monitoring and temperature measurement and can be fully integrated into high energy X-ray beam lines (such as at sector 6 at the APS).

In aerodynamic levitation, the sample is suspended in a stream of flowing gas. This means that when cooled heterogeneous nucleation can be avoided and it is often possible to cool samples to the point of vitrification. Diffraction data can therefore be obtained, in principle from stable liquids, supercooled liquids and glasses during this vitrification process. Recently, there has been significant technical progress that enables rapid acquisition of diffraction data by using a fast large area detector, measurements can be made at a rate of 5 Hz and the structure of liquids in transient, super-cooling conditions studied. The detector is configured to collect data in triggered mode such that the laser heating the sample is blocked or regulated to a given cooling rate, to quench the sample and a series of frames can be collected as the liquids are vitrified. The imaging control program is set up to allow continuous data scanning. The controlled program can be triggered to allow a fast burst of data to be buffered in memory and then written to disk. This arrangement allows blocks of up to ~50 images to be acquired in a period of a few seconds. The data collection is synchronised with the laser operation and data can be collected during the quenching of the liquid. The high flux at sector 6 allows full diffraction patterns to will be collected in as little as 200 ms. The data are then reduced and the process of vitrification therefore studied directly.

The liquid drop is levitated by a gas jet in the aerodynamic levitation furnace. Argon or oxygen are typically used as this levitation gas but more recently, gas mixing has been introduced. This means that the composition of the gas can be changed and the partial pressure of oxygen in the levitating jet and sample chamber can be controlled. Liquids that contain mixed valence elements can therefore be studied, for example the introduction of gas-mixing (CO/CO_2) has allowed the partial pressure of oxygen to be controlled and the study of iron-, titanium- and cobalt-bearing liquids under controlled pO_2 can be undertaken.

2.3. Molecular dynamics

In the HEXRD studies completed to date it is clear that a detailed interpretation of the liquid and glassy diffraction patterns cannot be effectively made without an adequate structural model. Recent work on molten salts has demonstrated the effectiveness of a combined HEXRD/molecular dynamics simulation approach For the simulation results presented here for molten salts we have used potentials of the Born-Mayer form [16] to account for short range interactions. For liquids with molecular anions we have adopted an approach that allows the molecular anions to be flexible by joining O-O pairs and M-O pairs within a given anion with harmonic springs. In addition we have developed a methodology that aims to understand and replicate the

intramolecular charge distribution. By adopting this approach there is the potential to model mixtures of different molecular anions by using a single model which controls both anion charge distribution and anion flexibility. In simulations (of molten salts) we have adopted the strategy of surveying experimental data and simulation results in reciprocal space before focusing on the simulation results to obtained detailed information in real space. This approach reflects the fact the diffraction data are obtained in reciprocal space and the analogous information can be obtained directly from the atom positions for the simulation with the total scattering functions constructed from the underlying partial structure factors. In the systems we have studied the high Q regime is dominated by the geometrically well-defined molecular anion and reflects its flexibility. Obtaining lower Q information requires reliable simulation that may reveal detailed structural information masked in the experimentally-determined total scattering functions. Typically the simulations utilise systems of 512–1296 molecules in an NVT ensemble with the system densities constrained by reference to standard sources. Temperatures are controlled by using the Nosé-Hoover thermostats. The total scattering functions are generated by combining the Ashcroft-Langreth partial structure factors generated from the Fourier components of the ion densities. The weighted sums of these partial structure factors are combined to construct the total structure factor with the X-ray form factors taken from standard sources.

3. Results

The applications of these various methods are described below for three example systems. We illustrate the role of gas mixing when applied to a mixed valence system for iron-bearing silicate systems while some recent studies on tellurite systems are used to illustrate the potential for rapid data acquisition. Finally we use some examples of molten salts to demonstrate the potential for combining simulations with HEXRD to understand the structure and dynamics of fragile liquid systems.

3.1. Iron-bearing liquids

Iron is an important component of liquids and a series of studies has been undertaken to evaluate iron's structural roles in silicate liquids. These are important geologically and also, as slags, in the steel industry. Iron can potentially adopt different structural roles depending on valance state and requires that the partial pressure of oxygen be controlled. The introduction of gas mixing allows the pO$_2$ to be controlled and this combination of containerless methodology has been applied, with HEXRD, to simple silicate systems.

Fayalite composition liquids have been studied by Alderman et al. [17]. Here HEXRD has been combined with X-ray absorption spectroscopy measurements. The structure of the fayalite liquid however shows only very subtle changes with pO$_2$. In the real space transform, there is a single Fe-O correlation centred at 2.0 Å and provides the Fe-O coordination number of 4.4 to 4.7. Peak fitting routines have been used to deconvolute this correlation and indicate that most of the iron in this liquid is five coordinated by oxygen with some iron in higher (six-fold) coordination. There is only a very limited change in the in n_{FeO} with pO$_2$ and, therefore Fe^{3+} content. This seems to contradict the convention view of the role of the iron in silicate liquids where Fe^{2+} is viewed as a network-modifier and is coordinated by six oxygens while Fe^{3+} is believed to have tetrahedral coordination and acts as a network former. X-ray Absorption Near Edge Structure (XANES) spectra collected at the Fe K-edge show pre-edge features with different centroid energies corresponding to different Fe^{3+} contents. These and all have similar total areas and lie intermediate between values expected for 4- or 6-fold Fe also indicating average Fe-O coordination numbers close to 5.0, in agreement with the HEXRD. The XANES data show a shift in the pre-edge peaks to higher E upon melt-quenching. Such changes imply oxidation during melt-quenching, supported by the Mössbauer
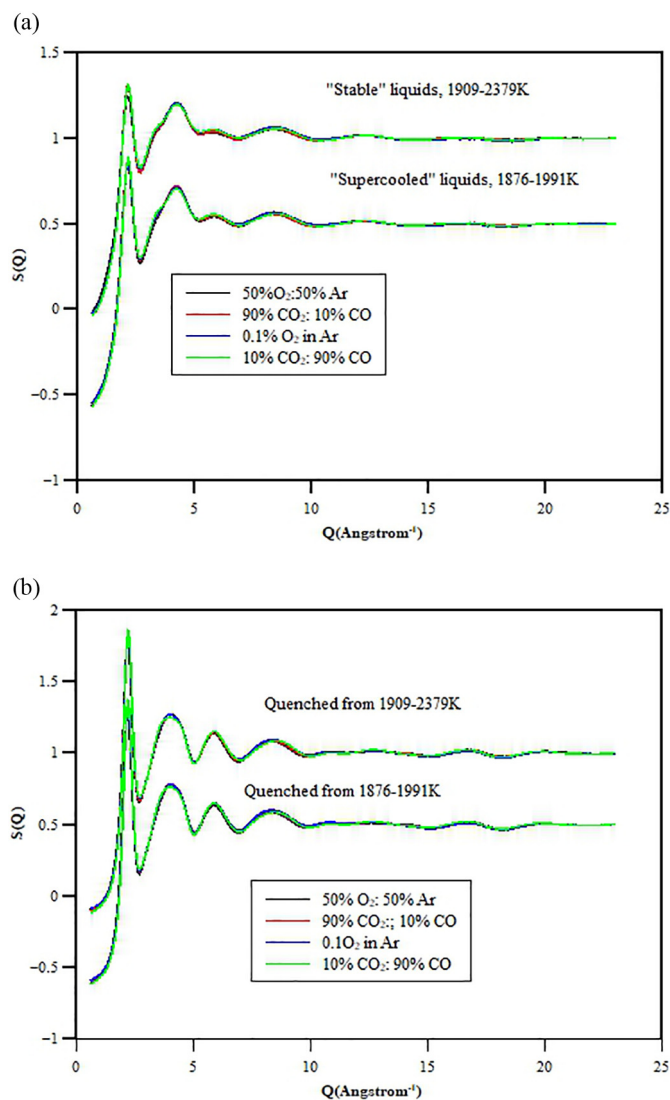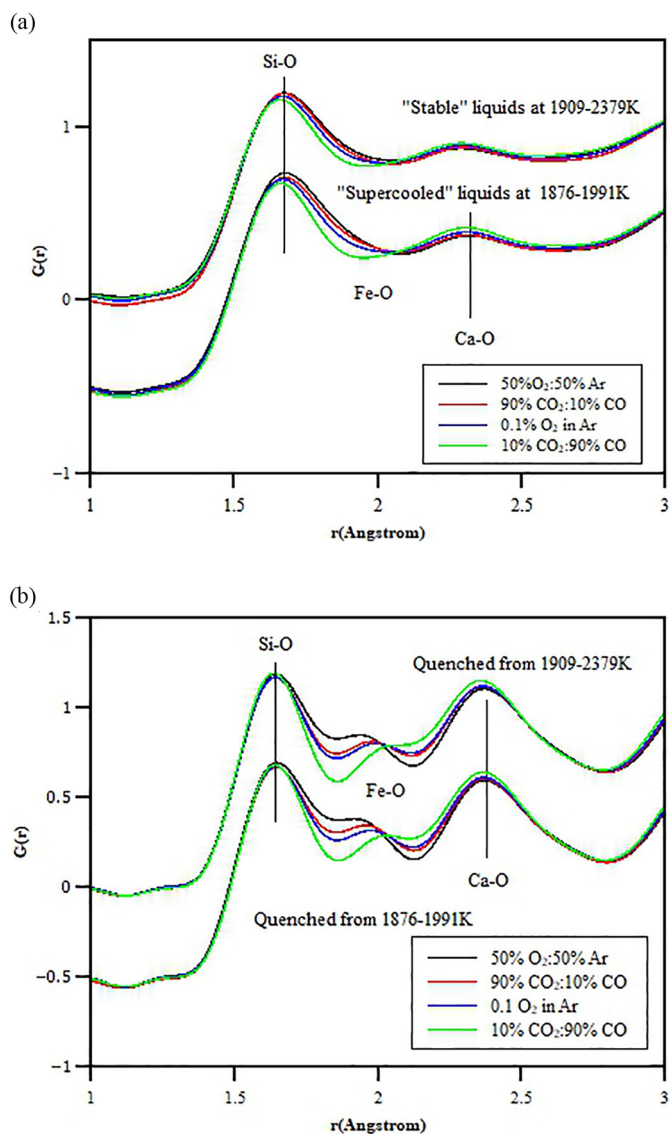
(a)

(b)

Fig. 1. HEXRD measurements (S(Q)) for levitated CaSiO$_3$ liquids (left) and glasses (right) with 20 mol% "FeO" levitated under different pO$_2$, controlled by the levitation gas.
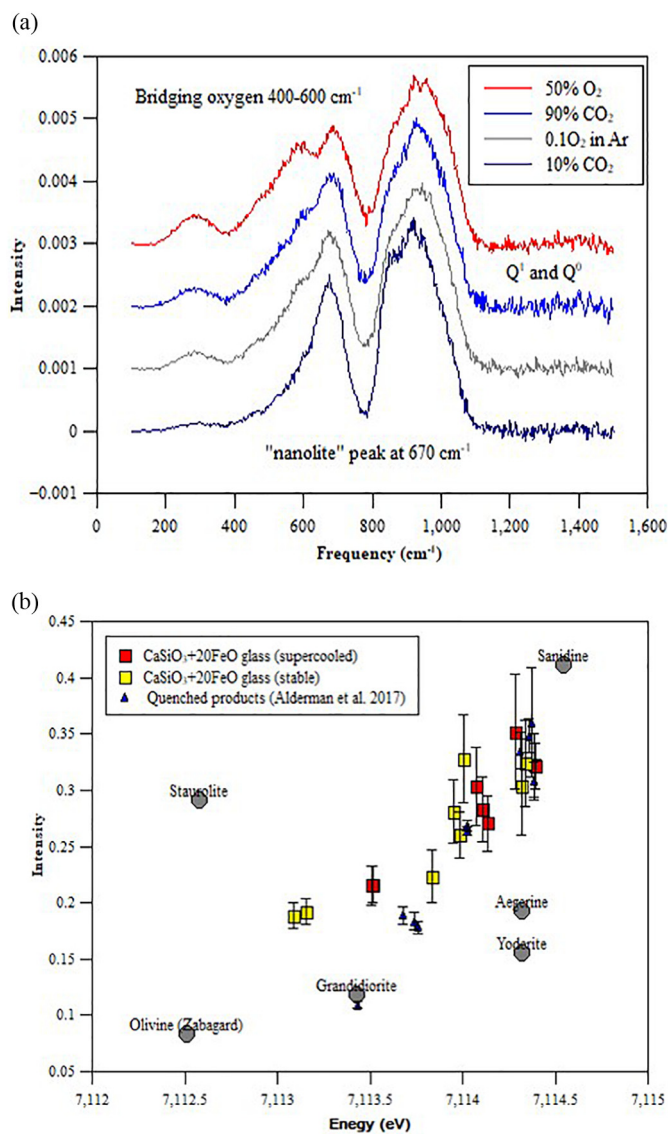
measurements on the recovered solids [17].

The simple slag system CaSiO$_3$ + "FeO" has been studied. A series of Fe-bearing calcium silicate liquids were studied using both HEXRD and XANES [18]. The latter data show differences in the Fe3 + content of liquids and glasses also suggesting oxidisation during the process of vitrification and this informed further investigation into these liquids with a composition of 20 mol% "FeO" studied. This system is glass forming and was studied over a wide range of pO$_2$, including pO$_2$ that buffered by CO:CO$_2$. HEXRD was collected for stable liquids and liquids supercooled ~300 K below the melting temperature. Glasses were quenched from the stable and supercooled liquids. The structure factors for these two sequences of liquids are shown in Fig. 1. There are subtle differences in the liquid structure as a function of ferric content but in real space the Fe-O correlation is shown to be broad with no resolution into separate Fe^{2+}-O and Fe^{3+} -O correlations possible. When quenched to glasses the resulting diffraction data show differences in structure that clearly depends on the thermal history. In some cases, when liquids have identical ferric contents different Fe^{3+}/ΣFe is quenched this is most obviously seen in the real space G(r) (Fig. 2) where the position of the Fe-O peak is clearly shifted to lower r in the more oxidised samples, these are cooled from the lower temperature. Although there is a shift in the centroid of this correlation the

(a)

(b)

Fig. 2. Real space transformed for levitated $CaSiO_3$ liquids (left) and glasses (right) with 20 mol% "FeO" levitated under different pO_2, controlled by the levitation gas and quenched from stable and metastable (supercooled) conditions. The Fe-O correlation is more prominent in the glass and shifts positon with ferric iron content. The Fe-O correlation can be fitted with a single Gaussian peak that indicates a coordination number of ~5. There is a change in Fe-O position but not coordination number with $Fe^{3+}/\Sigma Fe$.

(a)

(b)

Fig. 3. Micro Raman spectroscopy data collected from recovered glass samples (left) and μ-XANES measurements showing the changes in pre-edge features, compared to mineral standards. The Raman data suggest the presence of Fe-rich clusters (nanolites) while the XANES confirm limited change in coordination number.

coordination number is close to 5, this suggests the presence of 4-, 5- and 6- coordinate iron with 5-coordinate iron dominant. The recovered glass samples were analysed by micro-XANES, Raman spectroscopy and electron microprobe analysis (Fig. 3). There is no discernible difference in composition between the cores and rims of these glasses and micro-XANES shows only limited differences between core and rim suggesting that the liquid remain in equilibrium with the levitation gas on quenching. The Raman spectroscopy measurements show differences between glass structure, dependent on thermal history and show the notable presence of a so-called "nanolite" peak suggesting that iron forms clusters within the liquid [19,20]. This would suggest that there would be small-angle scattering at values of Q lower than currently accessible for these combined studies. Some preliminary studies on recovered glasses are inconclusive although "nanolite" clusters are identified in naturally occurring glasses with similar iron contents [19,21].

3.2. Tellurite systems

Textures formed in tellurite glasses are reminiscent of those formed in yttrium aluminate glasses and in the latter systems these textures are often cited as evidence for a polyamorphic transitions; a first order transition in the supercooled liquid that results in formation of two glasses of identical composition [22,23]. In the tellurite systems the textures produced comprise partly crystalline segregations identified as so called "anti-glass" which is in reality a disordered crystalline state that might be expected if liquids are rapidly cooled and crystallise [24–26]. In polyamorphic systems the structural changes are anticipated to occur in the deeply supercooled liquid regime and a study was undertaken to evaluate the structural changes that occur in supercooled tellurites. Pure TeO_2 does not form glasses easily but the addition of network modifying components such as Bi_2O_3- and Nb_2O_5 enable glasses to be produced.

High energy X-ray diffraction data has been collected on series of glass-forming liquids in the system Bi_2O_3-Nb_2O_5-TeO_2 using the conical nozzle levitator and argon as a levitation gas. This example application

is used to illustrate the potential of fast data acquisition with diffraction data collected as the liquids are quenched for form a glass.

The HEXRD studies of the glasses do not suggest any link between these two phenomena, ternary glasses in the Bi_2O_3-Nb_2O_5-TeO_2 system reveal a glassy network based on interconnected TeO_4 and TeO_3 units that appears to remain relatively unchanged from the parent TeO_2 system [27,28]. The diffraction data are dominated by Te-Te correlations at distances greater than those found in pure TeO_2 phases but correspond to those for crystalline tellurites containing modifier cations. To explore this system further, liquids in the ternary system have been studied in both the stable liquid regime and, by using rapid data acquisition, as the liquids quench. The goals are to evaluate the differences in structure on vitrification and also to establish whether there are structural changes in the deeply supercooled regime that correlate with suggested polyamorphic transitions.

Diffraction data has been obtained for a series of liquid s in the Bi_2O_3-Nb_2O_5-TeO_2 system. These include the "antiglass" composition (85.76 TeO_2 7.14 Bi_2O_3 7.14 Nb_2O_5) and a more TeO2-rich liquid (90% TeO_2). Diffraction data was collected as these two liquids were quenched to form a glass. Liquids with lower TeO2 could not be quenched to form glasses and are completely crystalline when rapidly quenched. The

90% TeO_2 sample shows the growth of Bragg peak but is mainly glassy. The S(Q) data collected as these liquids were quenched is shown in Fig. 4. This illustrates the quality of data achievable at sector 6 using combined HEXRD and containerless technique.

The S(Q) for these compositions are dominated by Te-Te and Te-O correlations and the changes with intensity of the peaks in the S(Q) as the liquid is cooled will reflect changes in the underlying TeO_2 network during vitrification. The first peak in the diffraction pattern occurs at $2\,\text{Å}^{-1}$. This principal peak can be associated with spatial correlations over the medium range length-scale. This first peak can be identified as Te…Te correlations occurring with real space periodicity $2\pi/Q = \sim3–4\,\text{Å}$. The first peak in the diffraction pattern shows shifts to higher values of Q on cooling for the "antiglass" liquid and the increase in peak height is not linear with temperature. In previous studies of CaSiO3 we have correlated such changes with the development of clustering in the deeply supercooled regime. This non-linear increase in peak height as temperatures are decreases shows an inflection at ~1.1 Tg that could reflect the onset of non-ergodic liquid behaviour, this mimics the viscosity temperature behaviour in these fragile liquids. There is however no indication of a discontinuity in the supercooled liquid structure in the "antiglass" compositions that is reported in the
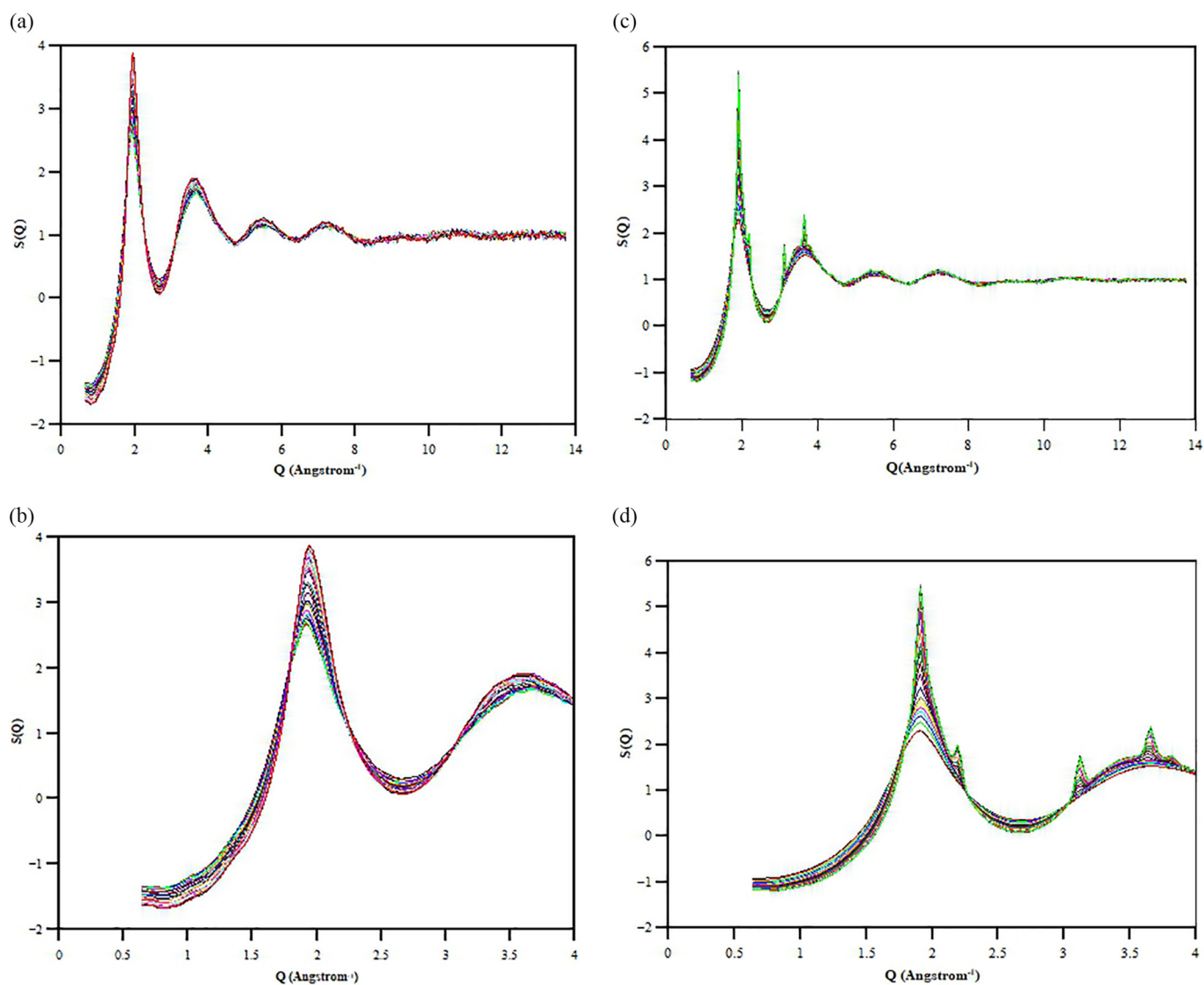
(a)

(c)

(b)

(d)

Fig. 4. HEXRD data collected for tellurite liquids collected form liquid and quenched to form a glass. The top panels are for the so-called anti glass composition (85.76 TeO_2 7.14 Bi_2O_3 7.14 Nb_2O_5). There are changes in intensity of the first peak and shift to higher Q on cooling (top right) but no direct evidence for a discontinuity in structure. The 90% TeO_2 liquid (bottom) partly crystallises on cooling.

Y_2O_3-Al_2O_3 system and this indicates that for this system, if a liquid-liquid transition is present it is below the calorimetric glass transition and can only be accessed by reheating previously quenched samples [29].

3.3. Molten salts

A detailed interpretation of the liquid and glassy diffraction patterns cannot be made without some form of structural model which is required to evaluate the partial structural contributions to the total scattering patterns in both reciprocal space and their real space transforms. Although the examples discussed below are liquids and not glass-forming they do illustrate the significant insight into the structure of apparently simple liquids and also the more detailed understanding of properties such as liquid fragility that can be achieved by allowing parameters such as temperature to vary.

A series of alkali molten salts have been studied, these include nitrates, nitrites, carbonates sulphates, and more recently phosphates [30–32]. Molten salts of this type have been traditionally regarded as simple ionic liquids comprising molecular anions with alkali cations. These liquids have been most commonly modelled by assuming the molecular anion to be rigid. However spectroscopic studies suggest that these anions are relatively flexible. In addition, many simulations of molten salts are limited by the lack of experimental data, so the combination of containerless methodologies, HEXRD and classical MD simulations has been shown to provide significant insight into the structure of these apparently simple liquids. The flexibility of the anion can be constrained by considering the high Q parts of the total structure factor while detail on the intermediate range order is available at lower Q. In Fig. 5 the diffraction data for a series of molten alkali sulphates are shown, as the identity of the alkali cation is changed the information in the diffraction pattern is changed. For Rb_2SO_4 the rubidium dominates that scattering whereas in Li_2SO_4, lithium only scatters X-rays weakly so the diffraction pattern is dominated by the S-S, S-O and O-O correlations from the SO_4 anion. A prominent feature in the diffraction pattern is the peak at $1.5\,\text{Å}^{-1}$. As with our studies of carbonates, the sulphate liquid can be modelled by allowing harmonic springs to control the O-O and S-O interactions, these can be varied to match the high Q-part of the diffraction pattern (dominated by the short range order of the SO_4^{2-} tetrahedron) and the low Q part where S-S, S-O and O-O also dominate. There is no evidence however for the formation of chains or the development of secondary length scales in these sulphate liquids. The first peak is shown for arise from the S-S pairs (Fig. 5) does with a periodicity on the length scale of 4–5 Å where (2π/Q) which most likely reflects the spherical nature of the sulphate unit with the SO_4^{2-} groups acting as large spheres.

The same basic model has been to simulate molten alkali nitrates and nitrites. In this example, not only are the NO_3^- and NO_3^- anions allowed to be flexible but charge is allowed to fluctuate across the anion [31]. The flexibility of the anions allows out-of-plane polarization to occur for the planar anions, one consequence of this is the emergence of a temperature-dependent length scale, as identified in studies of carbonate although neither nitrates nor nitrites show evidence for formation of polymerised units. The temperature-dependent development of an emergent length scale effects on nitrates and nitrites is seen most obviously in real space, there are changes in N-O and O-O ordering on the inter-molecular length scale in nitrates as a function of temperature with the partial contributions shifting to lower values of radial distance as temperature is reduced. In nitrites the behaviour is similar but with the additional development of a short length scale seen in the $g_{NN}(r)$. This indicates major structural differences between chemically related nitrate and nitrite liquids and, significantly this means that the nitrite structures cannot be formed from nitrates by removal of oxygen. The emergent length scales are different in the nitrates and nitrites and is a reflection of the charge balance on the respective molecular anions that results from the charge balancing model. The nitrites have a more
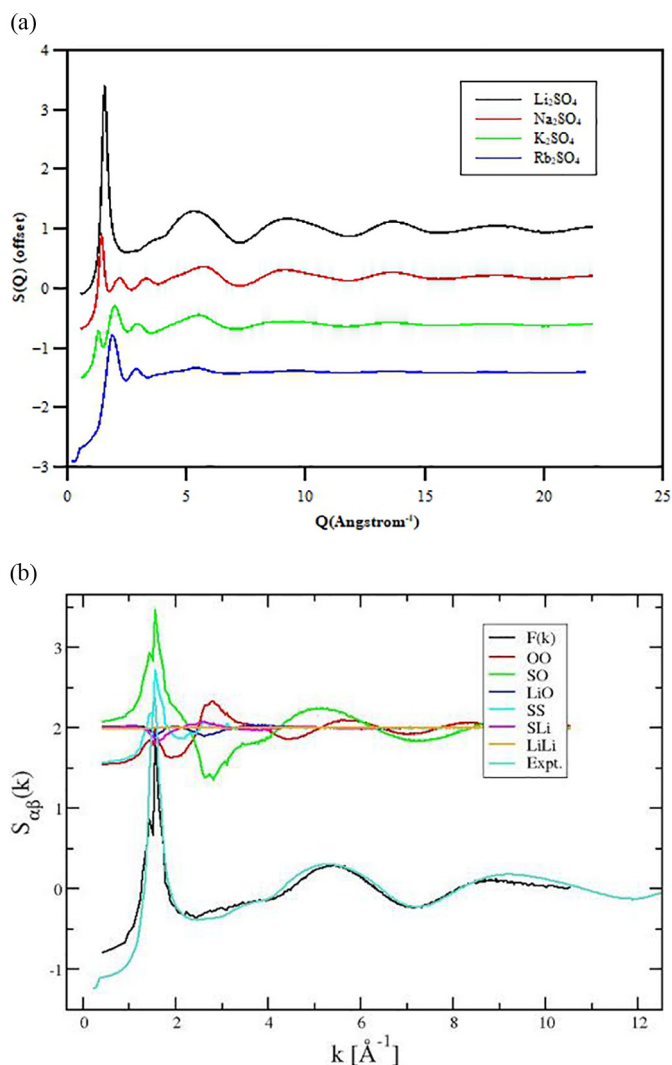
(a)

(b)

Fig. 5. Diffraction data for alkali sulfate liquids (left) and the Li_2SO_4 compared with the results of simulation (and the breakdown of the total structure factor into partial contributions shown at right.

prominent feature in the N-N distance reflecting the close approach of the NO_2^- pairs that is facilitated by the flexibility and charge-distribution of NO_2^- anions with dipoles formed by this molecular geometry pointing towards each other and forming this second length scale, this is less pronounced in the nitrates. The charge distributions also influence the distribution of cations surrounding the anion, specifically the degree of out of plane distortion which decreases as cation site increases.

Simulating these liquids with flexible anion geometry and fluctuating charge allows parameters such as temperature to be explored and transport properties such as diffusion, by extension viscosity, evaluated. This means that the fragility of liquids can be studied and in the case of carbonates for example, the combined approach of HEXRD and molecular dynamics with flexible anions and fluctuating change is used to correlate the changes in viscosity that occur in fragile liquids with the development of CO_3^{2-} chains and other linked structure as the carbonate liquids are cooled.

4. Conclusions

The combination of HEXRD and containerless techniques allows detailed structural information to be obtained as a function of composition over a wide range of temperatures and also as a function of pO_2.

This means that highly refractory and reactive liquids can be studied across phase diagrams with compositions not necessarily restricted to glass-forming liquids. The fast acquisition time means that the transient structures that form during supercooling can also be studied, up to the point of vitrification if the systems are glass-forming.

The combination of HEXRD and containerless methodology is illustrated above for three examples which highlight fast acquisition, the application of the combined techniques to systems with mixed valance components and the insight gained by combining these techniques with advanced simulation. All of these examples highlight the need to combine the diffraction with other techniques, either applied to samples recovered from liquid state studies or, ideally under similar conditions. All these studies are limited unless some modelling is performed to identify the partial structural contributions to the total scattering patterns and directed application of simulations can not only be used in combination with the diffraction data to further explore parameter space but can be used to identify key systems or conditions for study.

A recurrent theme in all of these studies outlined above is the emergence of length scales that exceed those probed in diffraction measurements. This would suggest that many properties of glass-forming liquids require a combination of scattering techniques that can identify the relative contribution to liquid dynamics from different length scales and would favour combinations of small and wide angle scattering is these liquid studies state studies. The ongoing development of high energy techniques at high flux sources such as the APS has potential to probe the development of both crystalline and amorphous nanoscale structures with overlapping small and wide angle detectors now available at sector 6 will enable continuous measurements over a range of Q space from $0.01\,\text{Å}^{-1}$ to a maximum value of ~15–$20\,\text{Å}^{-1}$. These provides the opportunity to expand the length scales studied and observed the formation of intermediate range structures in a variety of technically important liquids.

Declaration of competing interests

The authors declare that they have no known competing financial interests or personal relationships that could have appeared to influence the work reported in this paper.

Acknowledgements

References

[1] C.A. Angell, Formation of glasses from liquids and biopolymers, Science 267 (5206) (1995) 1924–1935.

[2] C. Le Losq, D.R. Neuville, Molecular structure, configurational entropy and viscosity of silicate melts: link through the Adam and Gibbs theory of viscous flow, J. Non-Cryst. Solids 463 (2017) 175–188.

[3] C.J. Benmore, X-ray diffraction from glass, in: M. Affatigato (Ed.), Modern Glass Characterization, 2015, pp. 241–270.

[4] M.C. Wilding, et al., Structural changes in supercooled Al2O3-Y2O3 liquids, Phys. Chem. Chem. Phys. 15 (22) (2013) 8589–8605.

[5] C.J. Benmore, et al., Temperature-dependent structural heterogeneity in calcium silicate liquids, Phys. Rev. B 82 (22) (2010).

[6] M.C. Wilding, C.J. Benmore, J.K.R. Weber, Changes in the local environment surrounding magnesium ions in fragile MgO-SiO2 liquids, Epl 89 (2) (2010).

[7] M.C. Wilding, C.J. Benmore, J.K.R. Weber, High-energy X-ray diffraction from Aluminosilicate liquids, J. Phys. Chem. B 114 (17) (2010) 5742–5746.

[8] O.L.G. Alderman, et al., Continuous structural transition in glass-forming molten Titanate BaTi2O5, J. Phys. Chem. C 120 (47) (2016) 26974–26985.

[9] O.L.G. Alderman, et al., Temperature-driven structural transitions in molten sodium borates Na2O-B2O3: X-ray diffraction, thermodynamic modeling, and implications for topological constraint theory, J. Phys. Chem. C 120 (1) (2016) 553–560.

[10] J.K.R. Weber, et al., Aerodynamic levitator for in situ x-ray structure measurements on high temperature and molten nuclear fuel materials, Rev. Sci. Instrum. 87 (7) (2016).

[11] O.L.G. Alderman, et al., Structure of molten titanium dioxide, Phys. Rev. B 90 (9) (2014).

[12] L.B. Skinner, et al., Molten uranium dioxide structure and dynamics, Science 346 (6212) (2014) 984–987.

[13] J.K.R. Weber, et al., Measurements of liquid and glass structures using aerodynamic levitation and in-situ high energy x-ray and neutron scattering, J. Non-Cryst. Solids 383 (2014) 49–51.

[14] A.P. Hammersley, et al., Two-dimensional detector software: from real detector to idealised image or two-theta scan, High Pressure Res. 14 (4–6) (1996) 235–248.

[15] Y. Ivanyushenkov, et al., Development and operating experience of a short-period superconducting undulator at the advanced photon source, Phys. Rev. Spec. Top. Accel. Beams 18 (4) (2015).

[16] J. Tissen, G.J.M. Janssen, J.P. Vandereerden, Molecular dynamics simulation of binary mixtures of molten alkali carbonates, Mol. Phys. 82 (1) (1994) 101–111.

[17] O.L.G. Alderman, et al., Local structural variation with oxygen fugacity in Fe2SiO4 + x fayalitic iron silicate melts, Geochim. Cosmochim. Acta 203 (2017) 15–36.

[18] O.L.G. Alderman, et al., Iron K-edge X-ray absorption near-edge structure spectroscopy of aerodynamically levitated silicate melts and glasses, Chem. Geol. 453 (2017) 169–185.

[19] D. Di Genova, A. Caracciolo, S. Kolzenburg, Measuring the degree of "nanotilization" of volcanic glasses: understanding syn-eruptive processes recorded in melt inclusions, Lithos 318 (2018) 209–218.

[20] D. Di Genova, et al., Effect of iron and nanolites on Raman spectra of volcanic glasses: a reassessment of existing strategies to estimate the water content, Chem. Geol. 475 (2017) 76–86.

[21] T.G. Sharp, R.J. Stevenson, D.B. Dingwell, Microlites and "nanolites" in rhyolitic glass: microstructural and chemical characterization, Bull. Volcanol. 57 (8) (1996) 631–640.

[22] P.F. McMillan, et al., Polyamorphism and liquid-liquid phase transitions: challenges for experiment and theory, J. Phys. Condens. Matter 19 (41) (2007).

[23] P.F. McMillan, et al., Polyamorphism and liquid-liquid phase transitiions in amorphous silicon and super-cooled Al2O3-Y2O3 liquids, in: H.E. Stanley (Ed.), Liquid Polymorphism, 2013, pp. 309–353.

[24] M. Tromel, et al., Formation and luminescence of lower symmetical tellurite anti-glass phases, J. Solid State Chem. 76 (2) (1988) 345–354.

[25] G. Blasse, et al., Luminescence of tellurite anti-glass phases, J. Solid State Chem. 63 (2) (1986) 148–153.

[26] A. Bertrand, et al., New transparent glass-ceramics based on the crystallization of "anti-glass" Spherulites in the Bi2O3-Nb2O5-TeO2 system, Cryst. Growth Des. 15 (10) (2015) 5086–5096.

[27] E.R. Barney, et al., Alkali environments in tellurite glasses, J. Non-Cryst. Solids 414 (2015) 33–41.

[28] E.R. Barney, et al., Terminal oxygens in amorphous TeO2, J. Phys. Chem. Lett. 4 (14) (2013) 2312–2316.

[29] M.C. Wilding, et al., Structural studies of Bi2O3-Nb2O5-TeO2 glasses, J. Non-Cryst. Solids 451 (2016) 68–76.

[30] M. Wilson, et al., Structure and liquid fragility in sodium carbonate, J. Phys. Chem. A 122 (4) (2018) 1071–1076.

[31] M.C. Wilding, et al., The structure of liquid alkali nitrates and nitrites, Phys. Chem. Chem. Phys. 19 (32) (2017) 21625–21638.

[32] M.C. Wilding, et al., Low-dimensional network formation in molten sodium carbonate, Sci. Rep. (6) (2016).